Cagin et al., Supplemental Material

Supplemental Tables

	TFAM overexpression	mitoXhoI expression
Da-Gal4 (ubiquitous expression)	First instar larval lethal.	Embryonic/early first instar larval lethal.
OK371-Gal4 (motor neuron expression) at 25^{o}C	Late pupal lethal/viable adults that die within one week.	Late pupal lethal.
OK371-Gal4 (motor neuron expression) at 29^{o}C	Late pupal lethal.	Pupal lethal.

Table S1. Viability of animals with the TFAM overexpression or mitoXhoI expression using the ubiquitous driver Da-Gal4, or the motor neuron driver OK371-Gal4.

		TFAM *o/e*		*ATPsyn-Cf6* RNAi	
Gene symbol	*Gene title*	*p-value*	*Fold change*	*p-value*	*Fold change*
snoRNA:Me28S-G2596	*ncRNA*	0.0012	8.25	0.0009	8.57
snoRNA:Psi18S-640g	*ncRNA*	0.0005	5.63	0.0006	8.14
CG15784	*CG15784*	0.0002	5.53	6.03E-05	10.6
CG31918	*CG31918*	0.0002	3.70	0.0006	4.37
ImpL3 (LDH)	*Ecdysone-inducible gene L3 (Lactate dehydrogenase)*	0.0020	3.58	0.0003	7.97
Thor	*CG8846*	0.0027	3.24	0.0006	5.83

CG13430	*CG13430*	0.0012	3.11	0.002	2.86
CG18343	*CG18343*	0.0004	3.04	0.002	2.76
CG2064	*CG2064*	0.0002	2.80	0.0001	3.81
CG31157	*CG31157*	0.0032	2.46	0.0005	4.29
FucTB	*CG4435*	0.0007	2.46	0.0003	2.5
CG42694	*CG42694*	0.0009	2.2	0.002	1.66
Arc1	*Activity-regulated cytoskeleton associated protein 1*	0.0001	2.16	6.11E-05	2.56
snoRNA:Psi18S-525c	*ncRNA*	0.004	1.87	0.003	2.36
CG7607	*CG7607*	0.002	1.87	9.01E-05	2.18

Table S2. Top 15 most upregulated genes in common between larval CNS tissue overexpressing TFAM or with knock-down of ATPsynCf6 in neurons using nSyb-Gal4. For full list see Supplemental Tables S3-5.

	n number		**Median lifespan**	
	Male	Female	Male	Female
Control	76	122	40	46
sima 832	101	120	47	46
sima 833	96	112	47	46
TFAM	39	42	28	21.5
TFAM*;sima 832*	62	65	46	44
TFAM*;sima 833*	63	70	33	46

Table S3. n numbers and median lifespan for lifespan assays in male and female flies.

Log-Rank (Mantel Cox) test			Male	Female	Male	Female
Control	vs	TFAM	p=0.0027	p<0.0001	*	*
Control	vs	TFAM*;sima 832*	p=0.0052	p=0.0053	*	*
Control	vs	TFAM*;sima 833*	p=0.5725	p=0.0238	ns	ns
TFAM	vs	TFAM*;sima 832*	p<0.0001	p=0.0002	*	*
TFAM	vs	TFAM*;sima 833*	p=0.0025	p<0.0001	*	*

Table S4. Statistical comparison for lifespan assays in male and female flies.

Primer	*Sequence*
Tfam.EcoRI.Fw	5'-GAGAGAGAATTCATGATCTACACCACAACA-3'
Tfam.XbaI.Rv	5'-GAGATCTAGACTATATATCTTTGGAGGCC-3'
mtCoI-F	5'-GAGCTGGAACAGGATGAACTG-3'
mtCoI-R	5'-TTGAAGAAATCCCTGCTAAATGT-3'
Gapdh1-F	5'-GACGAAATCAAGGCTAAGGTCG-3'
Gapdh1-R	5'-AATGGGTGTCGCTGAAGAAGTC-3'
XhoI-F	5'-GCTCATCATATATTTACCGTTGGA-3'
XhoI-R	5'-AAAATTTTAATTCCAGTAGGAACTGC-3'
Rpl4-F	5'-TCCACCTTGAAGAAGGGCTA-3'
Rpl4-R	5'-TTGCGGATCTCCTCAGACTT-3'
ATPsynCF6-F	5' -GGAACAGCTGCTGGATGG- 3'
ATPsynCF6-R	5'-AGCATTTGCAAAGGAAAATAAGA-3'
Sima-F	5'-CAAACCAAAGGAGAAAAGAAGG-3'
Sima-R	5'-CAGCCGAGAGTTCCATGAAT-3'

Table S5. List of primers used. Restriction enzyme sites are underlined.

Supplemental Datasets

Dataset S1. Genes with significantly altered expression (FDR=0.2%) in TFAM overexpressing larval CNS tissue in neurons using nSyb-Gal4. See associated spreadsheet.

Dataset S2. Genes with significantly altered expression (FDR=0.2%) in ATPsynCf6 RNAi larval CNS tissue in neurons using nSyb-Gal4. See associated spreadsheet.

Dataset S3. Genes with significantly altered expression (FDR=0.2%) in both TFAM overexpression and ATPsynCf6 RNAi larval CNS tissue in neurons using nSyb-Gal4. See associated spreadsheet

Dataset S4. Genes with significantly altered expression in TFAM overexpressing and ATPsynCf6 RNAi larval CNS tissue in neurons using nSyb-Gal4, which were also differentially regulated in tko mutant flies, pink1 mutant flies and cytochrome c oxidase Va (CoVa) knock-down S2 cells (1-3), as well as in the HIF-dependent transcriptional response in Drosophila larvae (4). See associated spreadsheet

Supplemental Materials and Methods

Immunofluorescence and imaging

For imaging of the larval NMJ, late third instar larvae were transferred to a Sylgard dish in a drop of PBS and pinned out at the anterior and posterior tips using micro-pins (Entomoravia), then the cuticle was cut open along the dorsal midline using iridectomy scissors (Fine Science Tools), pinned out with four additional pins and the body contents removed, leaving the CNS. The PBS was then replaced with 4% formaldehyde/PBS and incubated for 20 minutes at room temperature. Fixed larvae were then washed three times with PBS/0.1% Triton X-100 (VWR) (PBST) before blocking in PBST/5% normal goat serum (PBST-NGS) for an additional hour. Larvae were incubated with primary antibody overnight in PBST-NGS at 4°C. After four washes in PBST larvae were incubated for ninety minutes with secondary antibody at room temperature, washed four times with PBST and then mounted in Vectashield (Vectalabs) after removal of the CNS. Type IB NMJs on muscle group 4, segment A3, were imaged at 40x, 1024 pixel resolution. Primary antibodies were mouse anti-NC82 (DSHB, 1:30) and mouse anti-HRP-Cy3 (Stratech, 1:1000). The secondary antibody was Alexa546 anti-mouse (Invitrogen).

For TMRM and MitoTracker Green staining, larvae were dissected as for fixed preparations, but in a drop of Schneider's medium (Sigma). The medium was replaced with 20nm TMRM or 200nM MitoTracker Green (Invitrogen) and anti-HRP-Cy3 (1:200, Stratech) in Schneider's medium and incubated at room temperature in the dark for 20 minutes. For

TMRM this was then replaced with 5nm TMRM and the larvae were placed in a drop of 5nm TMRM surrounded by Vaseline on a slide, a coverslip placed over the larvae and imaged with a 40x oil immersion lens. For MitoTracker Green preparations were mounted in Schneider's medium.

For measurement of glutathione redox potential the dissection protocol was adapted from Albrecht et al. (2011) (5). Wandering third instar larvae were briefly placed in dH_2O to wash away excess food. In order to obtain preps of fully reduced larvae, dissections were carried out in 20mM dithiothreitol (DTT) and then left to incubate for 10 minutes. The DTT was then removed and replaced with 20mM n-ethylmaleimide (NEM) for an additional 10 minutes. After one rinse with PBS, the preps were fixed in 4% formaldehyde/PBS for 15 minutes. Once fixed, the preps were again rinsed in PBS and washed three times in PBST for 10 minutes. The preps were then incubated for 40 minutes with anti-HRP-Cy3 (1:1000 in PBST-NGS, Stratech), followed by three 10 minute washes in PBST and a final wash in PBS. The preps were then mounted on slides in Vectashield. The same procedure was repeated for preps of fully oxidised larvae, using 2mM diamide (DA) instead of DTT. Control and test larvae were not treated with DA or DTT but were directly dissected in 20mM NEM and left for 10 minutes. The rest of the procedure was the same as outlined above. Reduced, oxidised, control and test larvae were imaged on the same day as dissection and mounting.

For immunostaining larval CNS tissue was fixed for 30 minutes in 4% formaldehyde/PBS, then washed three times for 10 minutes in PBST and blocked in PBST-NGS for one hour, then incubated with primary antibody overnight in PBST-NGS at 4°C. After four washes of ten minutes in PBST the tissue was incubated for ninety minutes with the secondary antibody at room temperature, washed four times in PBST and then mounted in Vectashield (Vectalabs). The primary antibodies were rabbit anti-Drosophila TFAM (Abcam ab47548, 1:500), chicken anti-β galactosidase (Abcam ab9361, 1:1000) and rabbit anti-active-caspase 3 (Cell Signaling, 1:200). The secondary antibodies were Alexa594 anti-rabbit and Alexa555 anti-chicken (Invitrogen, 1:1000).

Supplemental Figure legends

Fig. S1. Analysis of TFAM expression in motor neuron cell bodies with mitochondrial dysfunction. Motor neuron cell bodies from control larvae (A), larvae overexpressing TFAM (B), or expressing *mitoXhoI* (C) in motor neurons using *OK371-Gal4* stained for TFAM expression (red). Punctate structures are mtDNA nucleoids. CD8GFP expression (green) was used to visualise motor neurons. Scale bar: 10µm. (D) Overexpression of *TFAM* with the motor neuron driver *D42-Gal4* causes reduced climbing compared to the control. For the box and whisker plot the horizontal line represents the median and whiskers represent the 5^{th} to 95^{th} percentile. ***$p \leq 0.001$. Controls are *Gal4* hemizygotes.

Fig. S2. Mitochondrial dysfunction does not cause motor neuron cell death. (A) Representative image of CD8GFP expressed in motor neuron cell bodies using *OK371-Gal4*. (B) Motor neuron cell bodies were quantified in control larvae, or in larvae overexpressing TFAM or expressing mitoXhoI in motor neurons using *OK371-Gal4.* Control n=5, TFAM overexpression n=3, mitoXhoI n=5. Data are represented as mean +/- SEM. Control are *OK371-Gal4* hemizygotes.

Fig. S3. Motor neuron specific mitochondrial dysfunction does not cause cell death. (A-C) Larval VNC from control larvae (A), larvae overexpressing TFAM (B), or expressing mitoXhoI (C) in motor neurons using *OK371-Gal4* stained for active-caspase 3 expression (red). (D,E) The VNC from control (D), or TFAM overexpressing (E) adult flies stained for active-caspase 3 expression (red). Expression of CD8-GFP (green) was used to visualise neuronal cell bodies.

Fig. S4. Motor neuron specific mitochondrial dysfunction causes defects in active zone development at muscle 6/7 NMJ. (A-C) Segment A3, muscle 6/7 NMJ in late third instar larvae from control larvae (A), larvae overexpressing TFAM (B), or expressing mitoXhoI (C) in motor neurons using *OK371-Gal4*. Expression of CD8-GFP (GFP) was used to visualise neuronal membranes and brp staining to visualise active zones. (D,E) Quantification of bouton number (D) and active zone number (E). Data are represented as mean +/- SEM, ***$p \leq 0.001$. Controls are *OK371-Gal4* hemizygotes.

Fig. S5. TMRM and Mitotracker Green staining of mitochondria in NMJs overexpressing TFAM or expressing mitoXhoI. Representative images from live preparations showing TMRM staining (red) in control (A), or NMJs overexpressing *TFAM* (B), or expressing *mitoXhoI* (C) in motor neurons using *OK371-Gal4*. Expression of CD8GFP (green) was used to visualise neuronal membranes. (D) Quantification of TMRM fluorescence intensity. Data are represented as mean +/- SEM. Control n=7, *TFAM* overexpression n=8, mitoXhoI n=8. (E-G) Representative images from live preparations showing Mitotracker Green staining (green) in control (A), or NMJs overexpressing TFAM (B), or expressing mitoXhoI (C) in motor neurons using *OK371*-Gal4. HRP (red) staining shows neuronal membranes. Controls are *OK371-Gal4* hemizygotes.

Fig. S6. Mitochondrial dysfunction causes progressive proximal to distal loss of mitochondria. (A-C) mitoGFP expression in equivalent motor neuron cell bodies in late third instar larval VNCs from control (A), or larvae overexpressing TFAM (B), or expressing mitoXhoI (C) using *OK371-Gal4*. (D-F) mitoGFP expression (green) in proximal motor neuron axons in late third instar larvae of the same genotypes as in (A-C). Horse radish peroxidase staining (red) shows neuronal membranes. (G-I) mitoGFP expression in distal motor neuron axons in late third instar larvae of the same genotypes as in (A-C). (J,K) Quantification of mitochondrial number (J) and volume (K) in proximal axons. (L,M) Quantification of mitochondrial number (L) and volume (M) in distal axons. Data are represented as mean +/- SEM, ***$p \leq 0.001$. Controls are *OK371-Gal4* hemizygotes.

Fig. S7. Neuronal mitochondrial dysfunction causes reduced mitochondrial glutathione redox potential. (A-E) Ratio images of mito-roGFP2-Grx1 fluorescence after excitation at 405nm (blue) and 488nm (green) in segment A3, muscle 4 NMJ in late third instar larvae from control larvae (A), control larvae treated with the reducing agent DTT (B), control larvae treated with the oxidising agent DA (C), larvae overexpressing TFAM (D), or expressing mitoXhoI (E) in motor neurons using *OK371-Gal4*. (F,G) Quantification of fluorescence emission ratio after excitation at 405nm/488nm. Data are represented as mean +/- SEM, *$p \leq 0.05$, **$p \leq 0.01$. Controls are *OK371-Gal4* hemizygotes.

Fig. S8. Motor neuron specific knock-down of ATPsynCf6 causes mitochondrial dysfunction. (A) qRT-PCR of *ATPsynCf6* mRNA levels from third instar larvae ubiquitously expressing a double stranded RNA against *ATPsynCf6* using *tub-Gal80^{ts}; tub-Gal4*. Control n=4, *ATPsynCf6* RNAi n=4. (B) Motor neuron specific knock-down of ATPsynCf6 using *D42-Gal4* decreases adult climbing ability. (C) Knock-down of ATPsynCf6 using *D42-Gal4* causes defective wing inflation. Control n=128, ATPsynCf6 n=44. (D,E) Motor neuron specific knock-down of ATPsynCf6 using *OK371-Gal4* causes loss of mitochondria at the larval NMJ. Motor neuron specific expression of mitoGFP (green) was used to visualise mitochondria and staining for horse radish peroxidise (HRP, red) to visualise neuronal membranes. (F,G) Quantification of mitochondrial number and volume. (H-K) Ratio images of mito-roGFP2-Grx1 fluorescence after excitation at 405nm (blue) and 488nm (green) in segment A3, muscle 4 NMJ in late third instar larvae from control larvae (H), control larvae treated with the reducing agent DTT (I), control larvae treated with the oxidising agent DA (J) and *ATPsynCf6* RNAi larvae (K) expressed in motor neurons using *OK371-Gal4*. (L) Quantification of fluorescence emission ratio after excitation at 405nm/488nm. For box and whisker plots the horizontal line represents the median and whiskers represent the 5th to 95th percentile. For bar graphs in (A),(F),(G) and (L) data are represented as mean +/- SEM. *p≤0.05, ***p≤0.001. Controls are *Gal4* heterozygotes.

Fig. S9. GO analysis, based on functional annotation clustering, of genes with significantly altered expression in TFAM overexpressing larval CNS tissue in neurons using nSyb-Gal4. Only clusters which included a count of gene number ≥ 10 are represented.

Fig. S10. GO analysis, based on functional annotation clustering, of genes with significantly altered expression in ATPsynCf6 RNAi larval CNS tissue in neurons using nSyb-Gal4. Only clusters which included a count of gene number ≥ 10 are represented.

Fig. S11. GO analysis, based on functional annotation clustering, of genes with significantly altered expression in TFAM overexpressing and ATPsynCf6 RNAi larval CNS tissue in neurons using nSyb-Gal4.

Fig. S12. Knock-down of Sima using an independent shRNA improves the function of neurons with mitochondrial dysfunction. (A) qRT-PCR of *sima* mRNA levels from third instar larvae ubiquitously expressing two independent shRNAs against *sima* using *Da-Gal4.* Control n=8, *sima* shRNA HMS00832 n=8, *sima* shRNA HMS00833 n=7. (B) Knock-down of *sima* (using shRNA HMS00832) improves the climbing ability of flies overexpressing TFAM using *D42-Gal4*. (C) Knock-down of Sima (using shRNA HMS00832) rescues the wing inflation defect of flies overexpressing TFAM using *D42-Gal4*. Control n=69, *sima* RNAi n=62, TFAM overexpression n=41, *sima* RNAi;TFAM overexpression n=34. $p<0.0001$. For box and whisker plot the horizontal line represents the median and whiskers represent the 5^{th} to 95^{th} percentile. For the bar graph in (A) data are represented as mean +/- SEM. *$p\leq0.05$, ***$p\leq0.001$. Controls are *Gal4* heterozygotes.

Fig. S13. Knock-down of Sima rescues the ATPsynCf6 RNAi wing inflation phenotype, does not affect the loss of NMJ mitochondria caused by TFAM overexpression but rescues the reduction in active zone number. (A) The *ATPsynCf6* RNAi wing inflation phenotype is rescued by knock-down of Sima using *D42-Gal4* ($p<0.0001$). Control n=224, *sima* RNAi n=130, *ATPsynCf6* RNAi n=58, *sima* RNAi; *ATPsynCf6* RNAi n=143. (B) The *ATPsynCf6* RNAi climbing phenotype is not affected by knock-down of Sima using *D42-Gal4*. (C-F') Segment A3, muscle 4 NMJ from control (C), *sima* RNAi (D), TFAM overexpression (E) and *sima* RNAi;TFAM overexpression (F) larvae using *OK371-Gal4.* Motor neuron specific expression of mitoGFP (green in C-F and white in C'-F') was used to visualise mitochondria and staining for horse radish peroxidise (HRP, red) to visualise neuronal membranes. (G) Quantification of mitochondrial volume. (H-K') brp expression in NMJs from control (H), *sima* RNAi (I), TFAM overexpression (J) and *sima* RNAi;TFAM overexpression (K) larvae using *OK371-Gal4.* Expression of CD8-GFP (GFP, green) was used to visualise neuronal membranes and brp staining (red in H-K and white in H'-K') to visualise active zones. For box and whisker plot the horizontal line represents the median and whiskers represent the 5^{th}

to 95th percentile. For the bar graph in (G) data are represented as mean +/- SEM. ***p≤0.001, n.s not significant. Controls are *Gal4* heterozygotes.

Supplemental References

1. Correia SC, *et al.* (2012) Mitochondrial importance in Alzheimer's, Huntington's and Parkinson's diseases. *Adv Exp Med Biol* 724:205-221.
2. Freije WA, Mandal S, & Banerjee U (2012) Expression profiling of attenuated mitochondrial function identifies retrograde signals in Drosophila. *G3 (Bethesda)* 2(8):843-851.
3. Schaefer AM, *et al.* (2008) Prevalence of mitochondrial DNA disease in adults. *Annals of neurology* 63(1):35-39.
4. Li Y, *et al.* (2013) HIF- and non-HIF-regulated hypoxic responses require the estrogen-related receptor in Drosophila melanogaster. *PLoS Genet* 9(1):e1003230.
5. Albrecht SC, Barata AG, Grosshans J, Teleman AA, & Dick TP (2011) In vivo mapping of hydrogen peroxide and oxidized glutathione reveals chemical and regional specificity of redox homeostasis. *Cell metabolism* 14(6):819-829.

Fig. S1

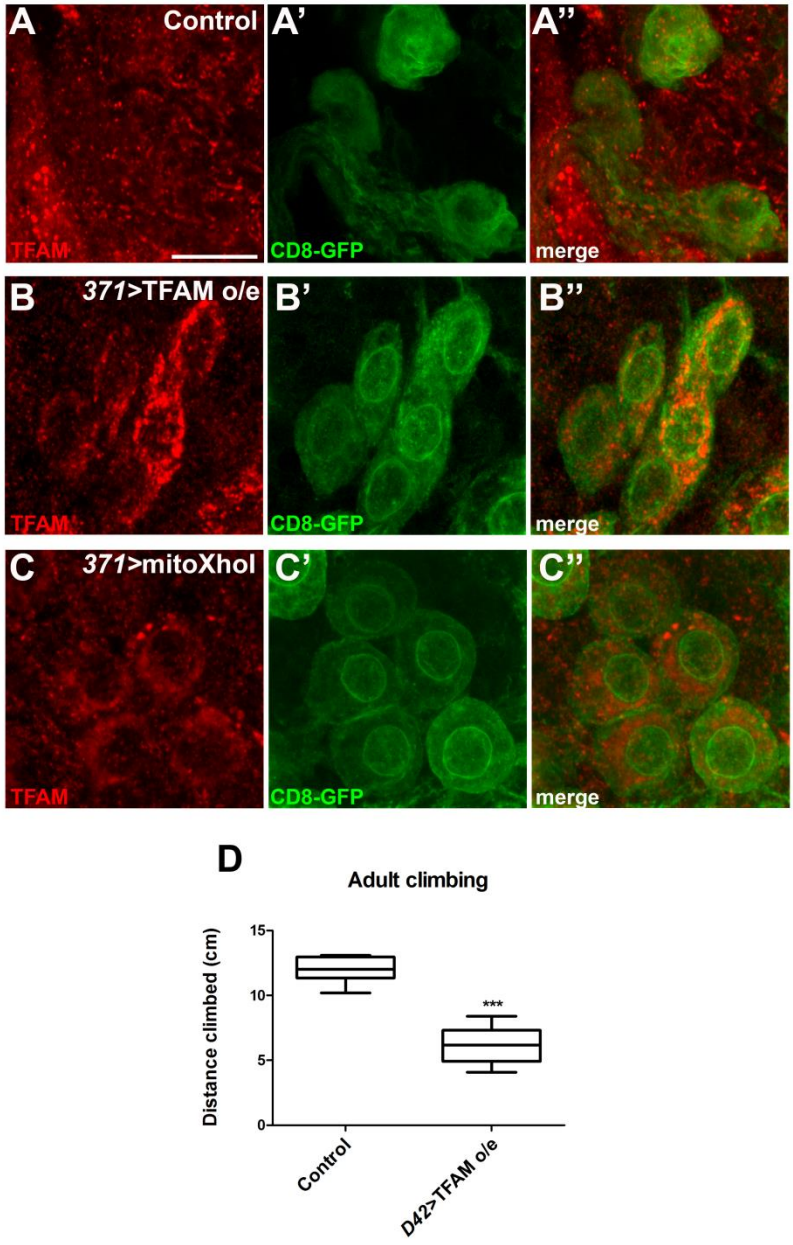
A
Control
A'
A''
TFAM
CD8-GFP
merge
B
371>TFAM o/e
B'
B''
TFAM
CD8-GFP
merge
C
371>mitoXhoI
C'
C''
TFAM
CD8-GFP
merge
D
Adult climbing
Distance climbed (cm)
15
10
5
0
***
Control
D42>TFAM o/e

Fig. S2

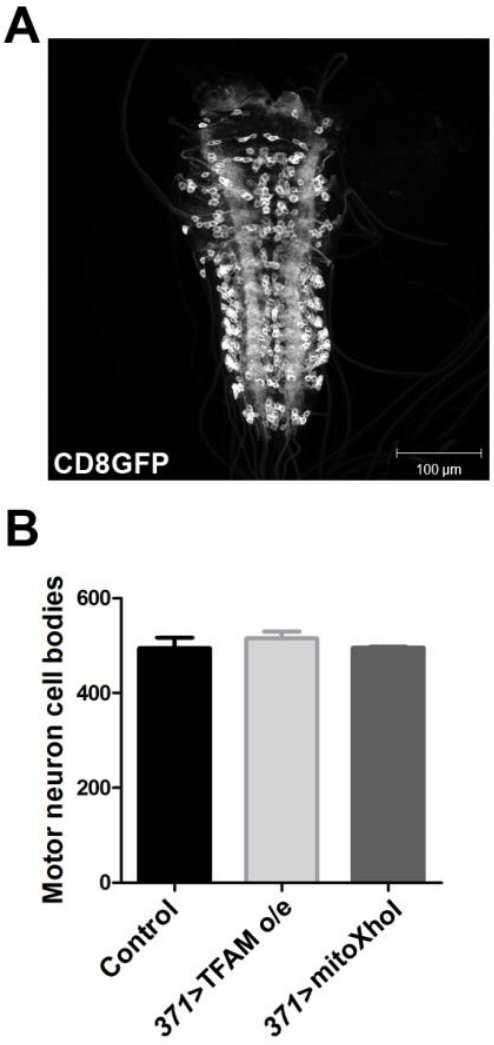
A
CD8GFP
100 µm
B
Motor neuron cell bodies
600
400
200
0
Control
371>TFAM o/e
371>mitoXhoI

Fig. S3

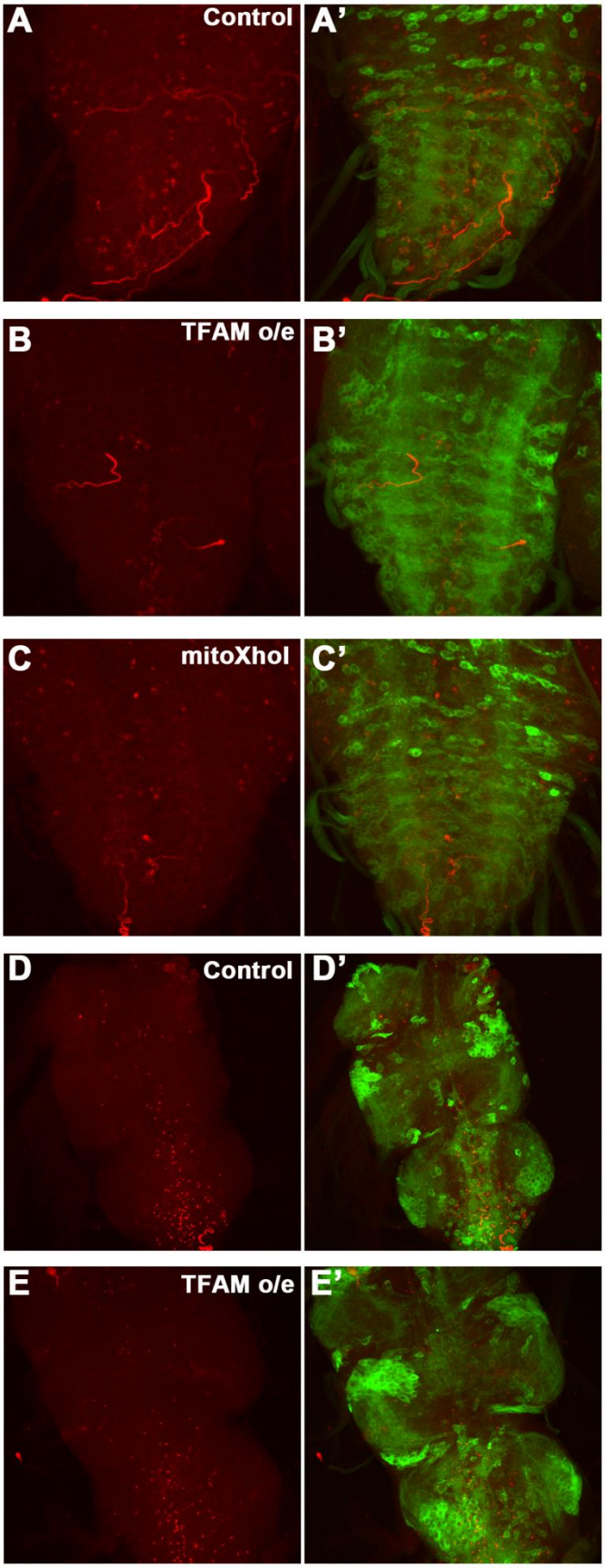

Fig. S4

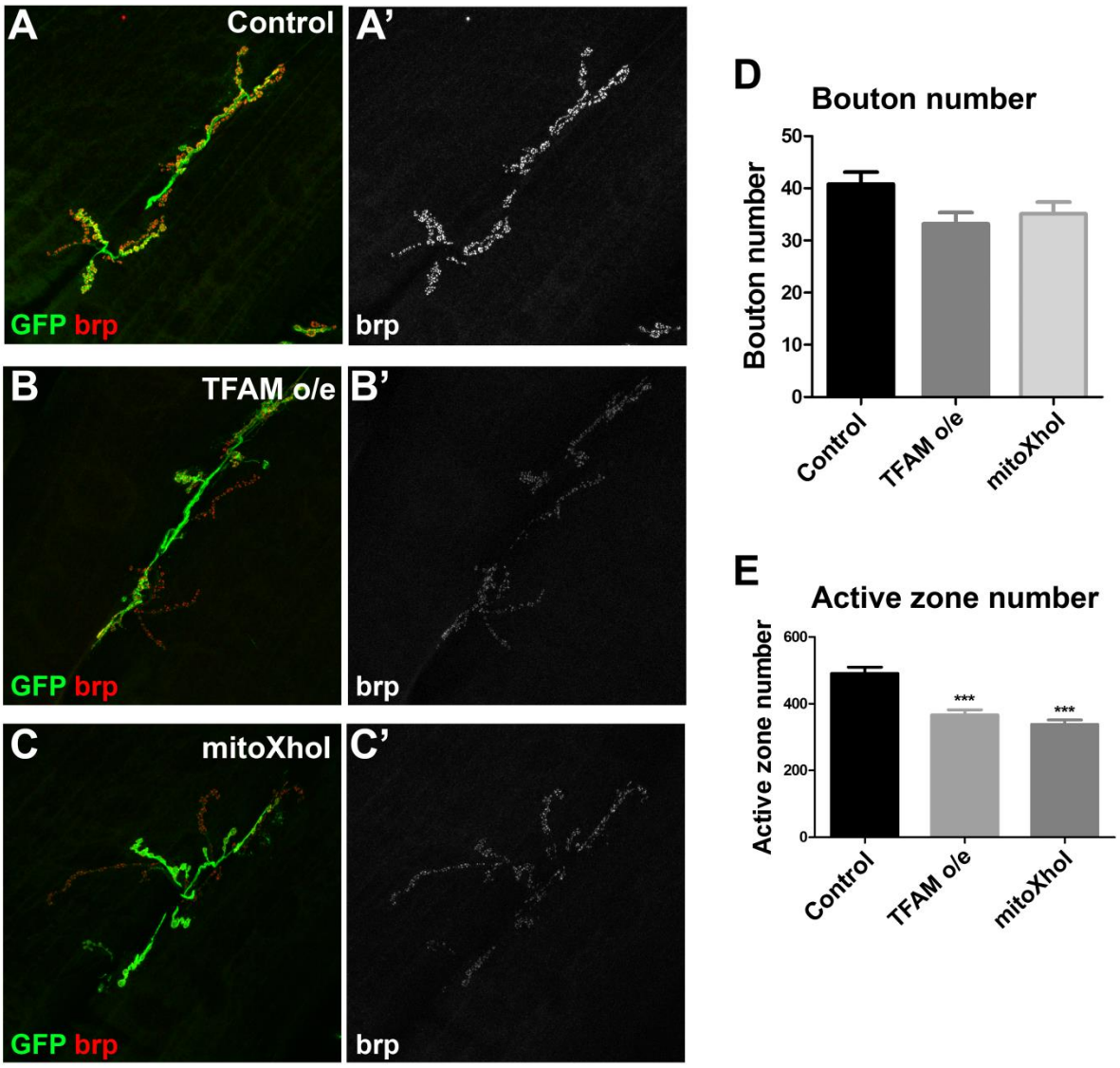
A
Control
GFP brp
A'
brp
B
TFAM o/e
GFP brp
B'
brp
C
mitoXhol
GFP brp
C'
brp
D
Bouton number
Bouton number
50
40
30
20
10
0
Control
TFAM o/e
mitoXhol
E
Active zone number
Active zone number
600
400
200
0
***
***
Control
TFAM o/e
mitoXhol

Fig. S5

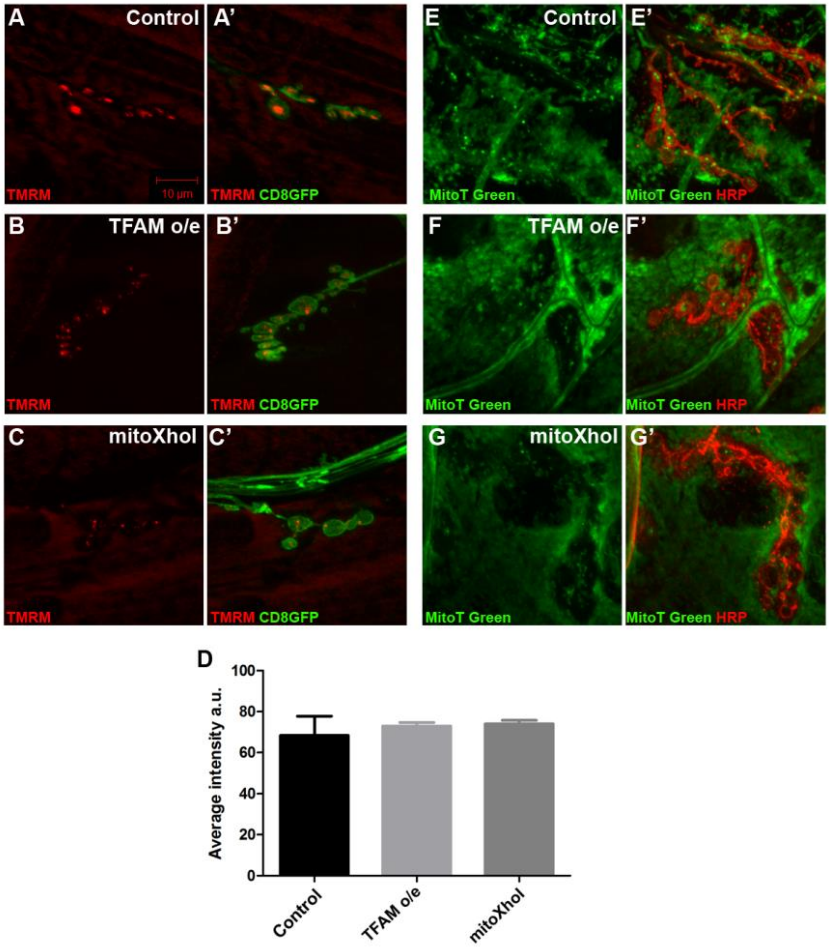
A
Control
A'
TMRM
10 µm
TMRM CD8GFP
E
Control
E'
MitoT Green
MitoT Green HRP
B
TFAM o/e
B'
TMRM
TMRM CD8GFP
F
TFAM o/e
F'
MitoT Green
MitoT Green HRP
C
mitoXhol
C'
TMRM
TMRM CD8GFP
G
mitoXhol
G'
MitoT Green
MitoT Green HRP
D
Average intensity a.u.
100
80
60
40
20
0
Control
TFAM o/e
mitoXhol

Fig. S6

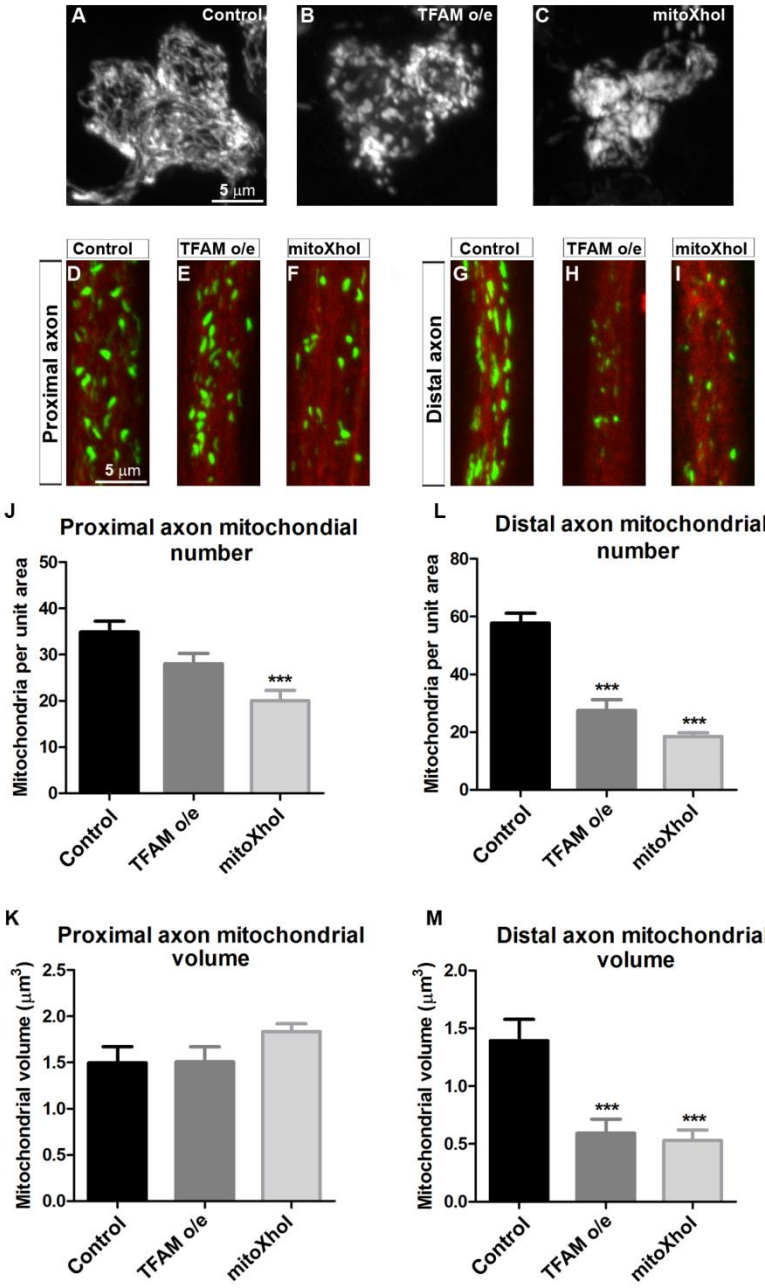
A
Control
B
TFAM o/e
C
mitoXhol
5 μm
Control
TFAM o/e
mitoXhol
Proximal axon
D
E
F
5 μm
Distal axon
G
H
I
J
Proximal axon mitochondial number
Mitochondria per unit area
***
Control
TFAM o/e
mitoXhol
L
Distal axon mitochondrial number
Mitochondria per unit area
***
***
Control
TFAM o/e
mitoXhol
K
Proximal axon mitochondrial volume
Mitochondrial volume (μm3)
Control
TFAM o/e
mitoXhol
M
Distal axon mitochondrial volume
Mitochondrial volume (μm3)
***
***
Control
TFAM o/e
mitoXhol

Fig. S7

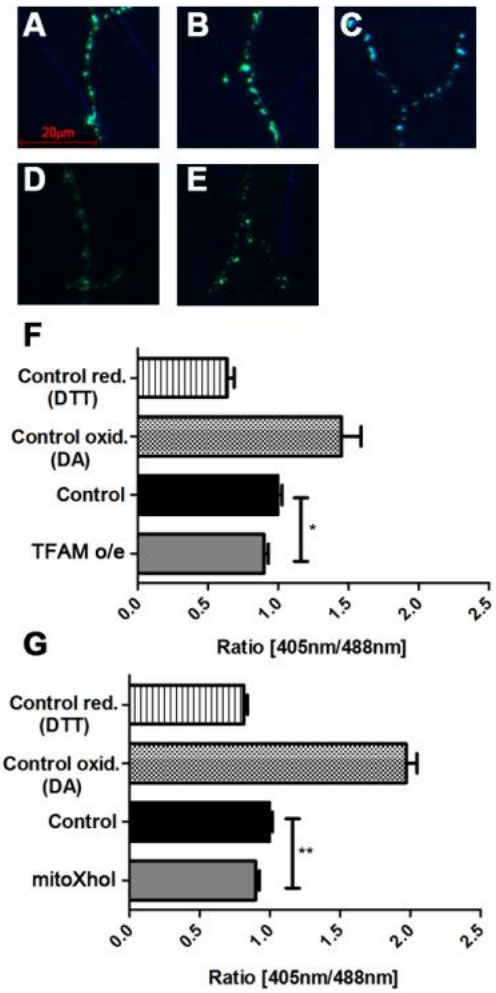
A
B
C
20µm
D
E
F
Control red. (DTT)
Control oxid. (DA)
Control
TFAM o/e
*
0.0
0.5
1.0
1.5
2.0
2.5
Ratio [405nm/488nm]
G
Control red. (DTT)
Control oxid. (DA)
Control
mitoXhol
**
0.0
0.5
1.0
1.5
2.0
2.5
Ratio [405nm/488nm]

Fig. S8

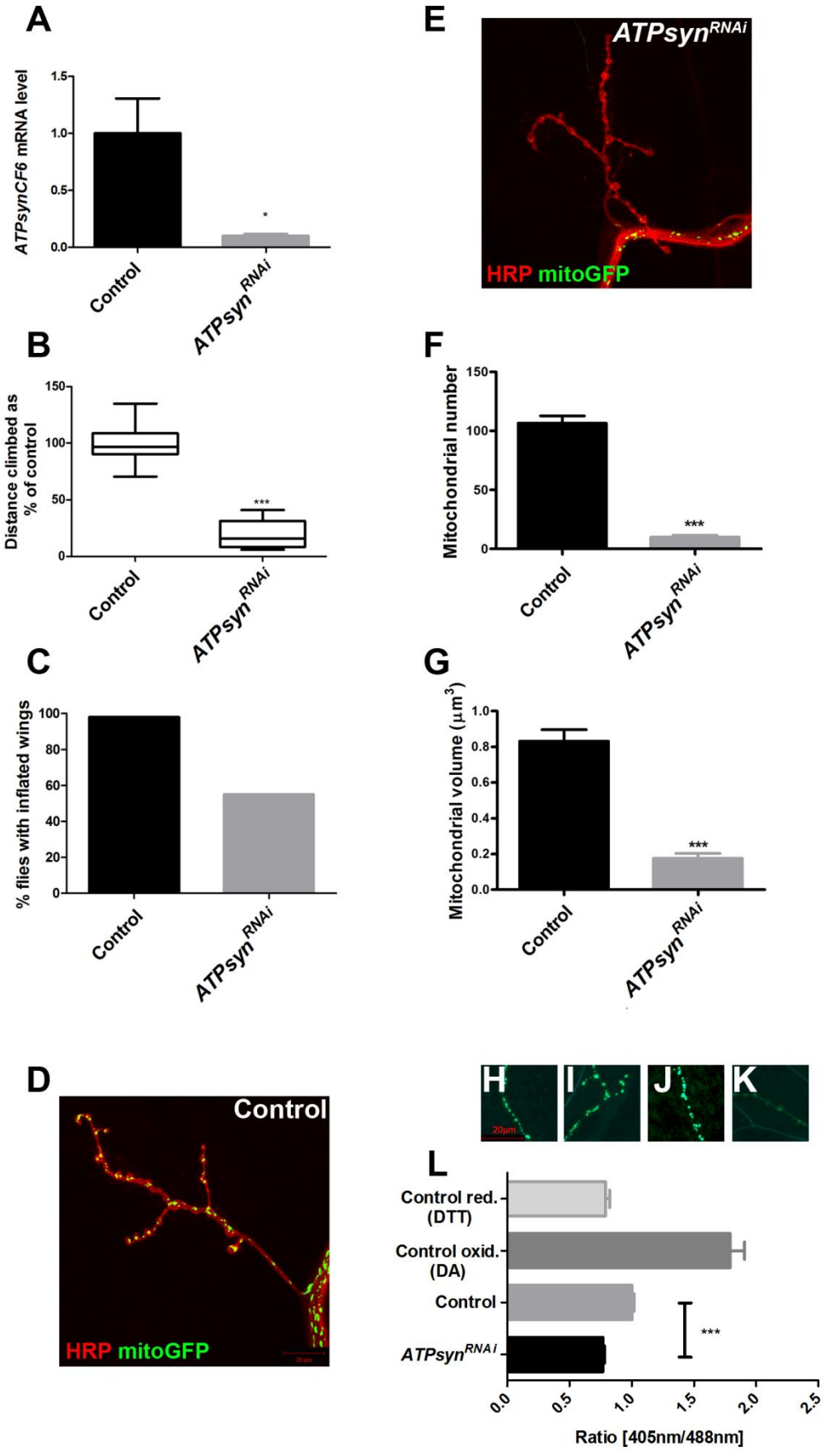
A
ATPsynCF6 mRNA level
1.5
1.0
0.5
0.0
*
Control
ATPsyn RNAi
B
Distance climbed as % of control
150
100
50
0
***
Control
ATPsyn RNAi
C
% flies with inflated wings
100
80
60
40
20
0
Control
ATPsyn RNAi
D
Control
HRP mitoGFP
E
ATPsyn RNAi
HRP mitoGFP
F
Mitochondrial number
150
100
50
0
***
Control
ATPsyn RNAi
G
Mitochondrial volume (µm3)
1.0
0.8
0.6
0.4
0.2
0.0
***
Control
ATPsyn RNAi
H
I
J
K
20µm
L
Control red. (DTT)
Control oxid. (DA)
Control
ATPsyn RNAi
***
0.0
0.5
1.0
1.5
2.0
2.5
Ratio [405nm/488nm]

Fig. S9

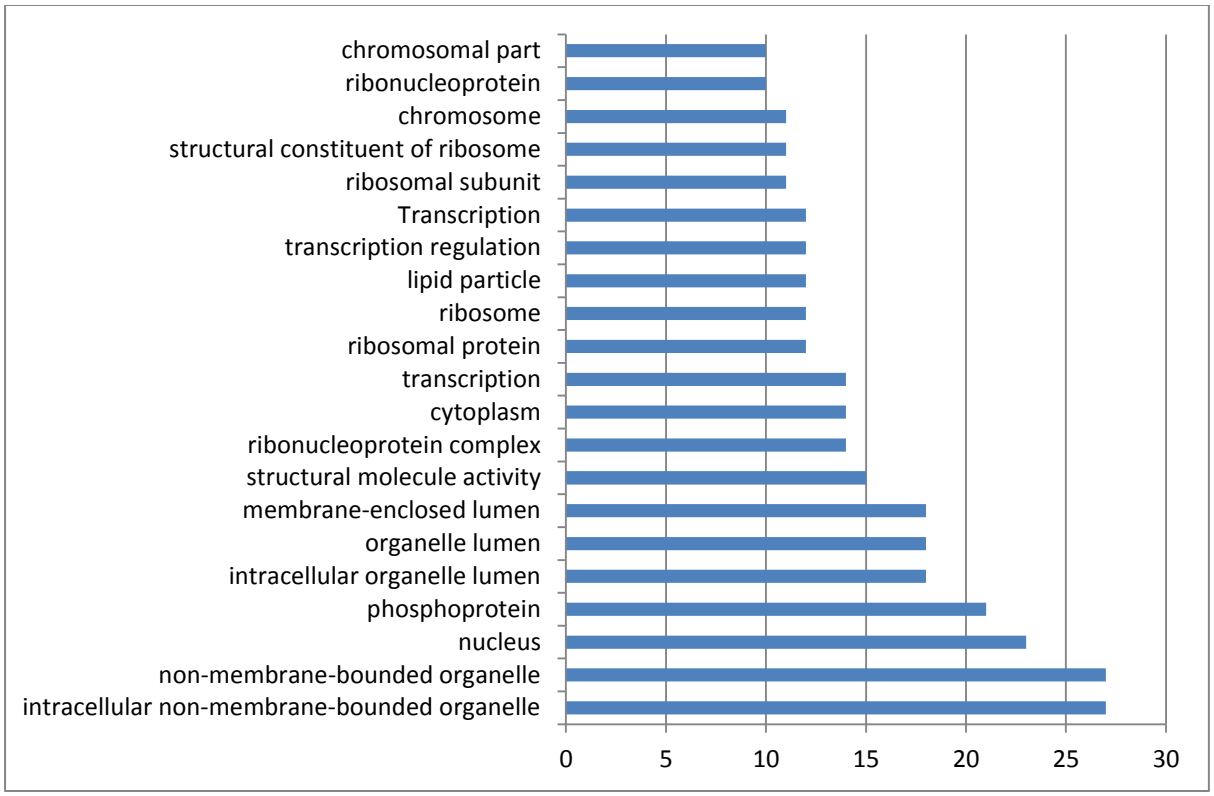
chromosomal part
ribonucleoprotein
chromosome
structural constituent of ribosome
ribosomal subunit
Transcription
transcription regulation
lipid particle
ribosome
ribosomal protein
transcription
cytoplasm
ribonucleoprotein complex
structural molecule activity
membrane-enclosed lumen
organelle lumen
intracellular organelle lumen
phosphoprotein
nucleus
non-membrane-bounded organelle
intracellular non-membrane-bounded organelle
0
5
10
15
20
25
30

Fig. S10

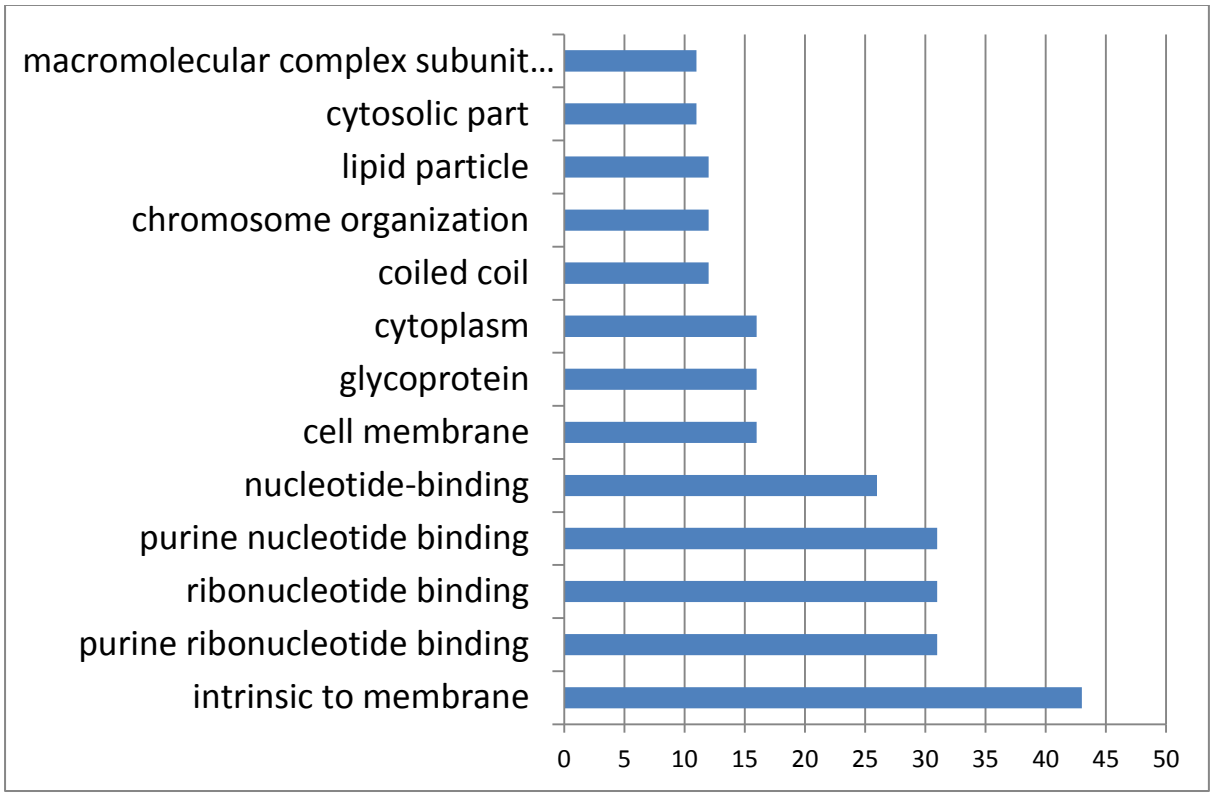
macromolecular complex subunit...
cytosolic part
lipid particle
chromosome organization
coiled coil
cytoplasm
glycoprotein
cell membrane
nucleotide-binding
purine nucleotide binding
ribonucleotide binding
purine ribonucleotide binding
intrinsic to membrane
0
5
10
15
20
25
30
35
40
45
50

Fig. S11

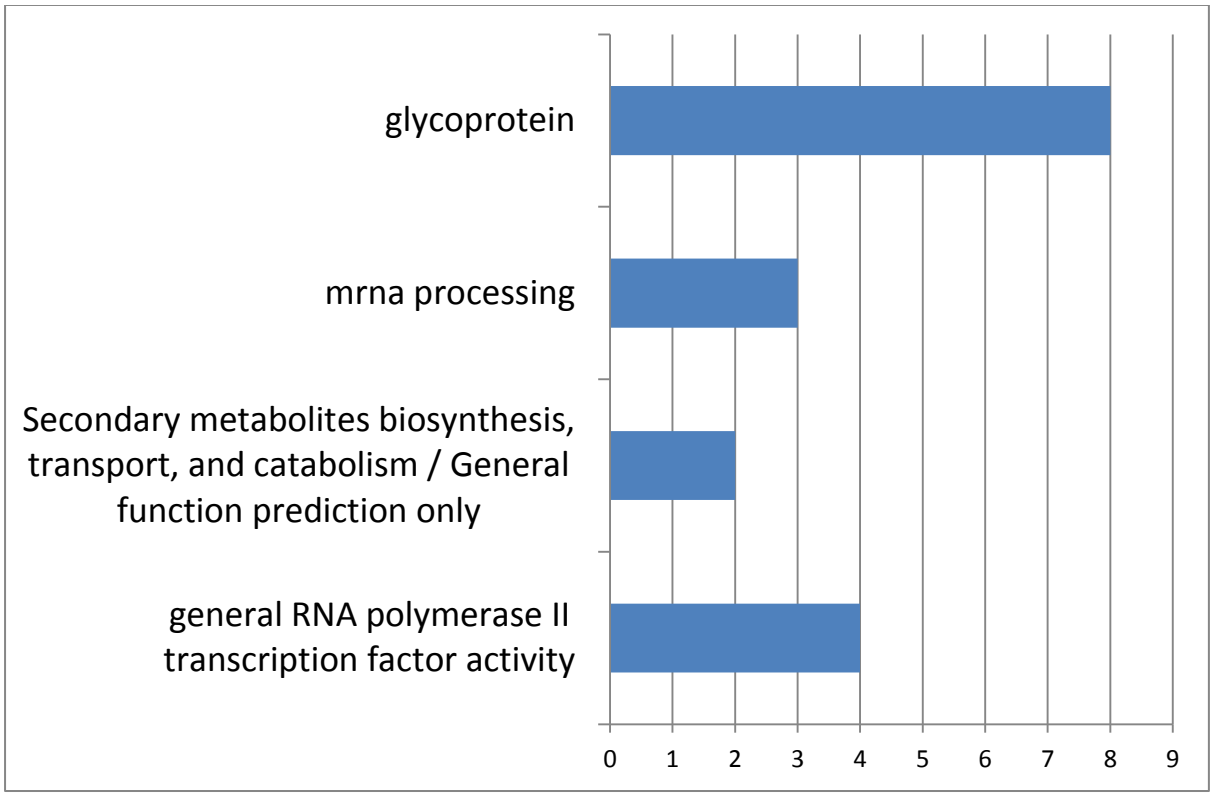
glycoprotein
mrna processing
Secondary metabolites biosynthesis, transport, and catabolism / General function prediction only
general RNA polymerase II transcription factor activity
0
1
2
3
4
5
6
7
8
9

Fig. S12

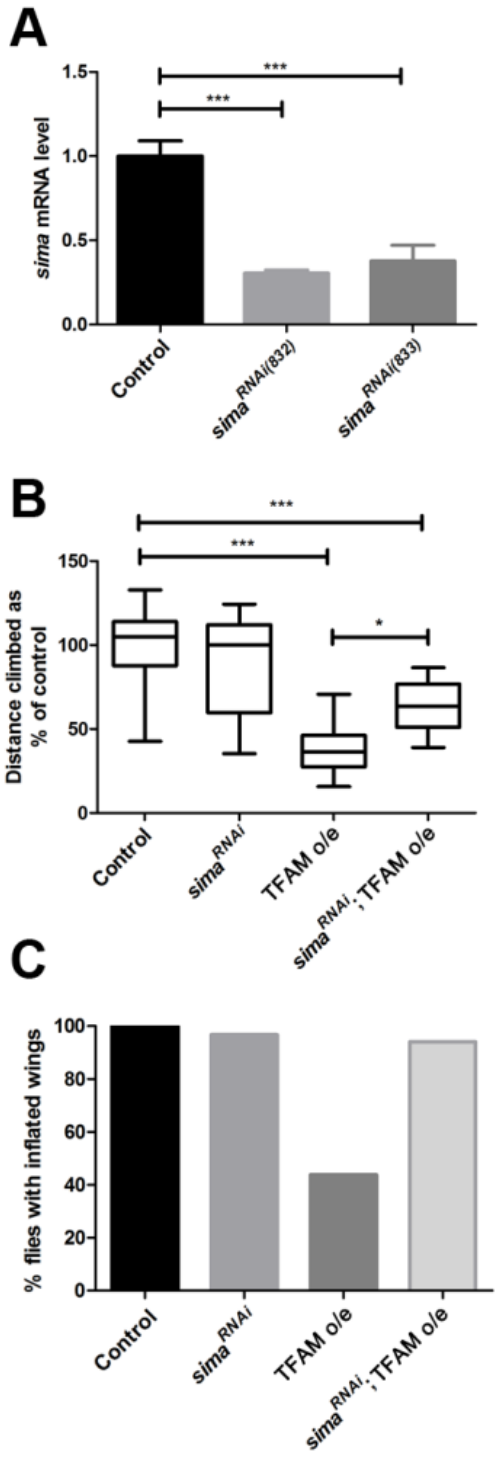
A
sima mRNA level
1.5
1.0
0.5
0.0
***
***
Control
sima RNAi(832)
sima RNAi(833)
B
Distance climbed as % of control
150
100
50
0
***
***
*
Control
sima RNAi
TFAM o/e
sima RNAi;TFAM o/e
C
% flies with inflated wings
100
80
60
40
20
0
Control
sima RNAi
TFAM o/e
sima RNAi;TFAM o/e

Fig. S13

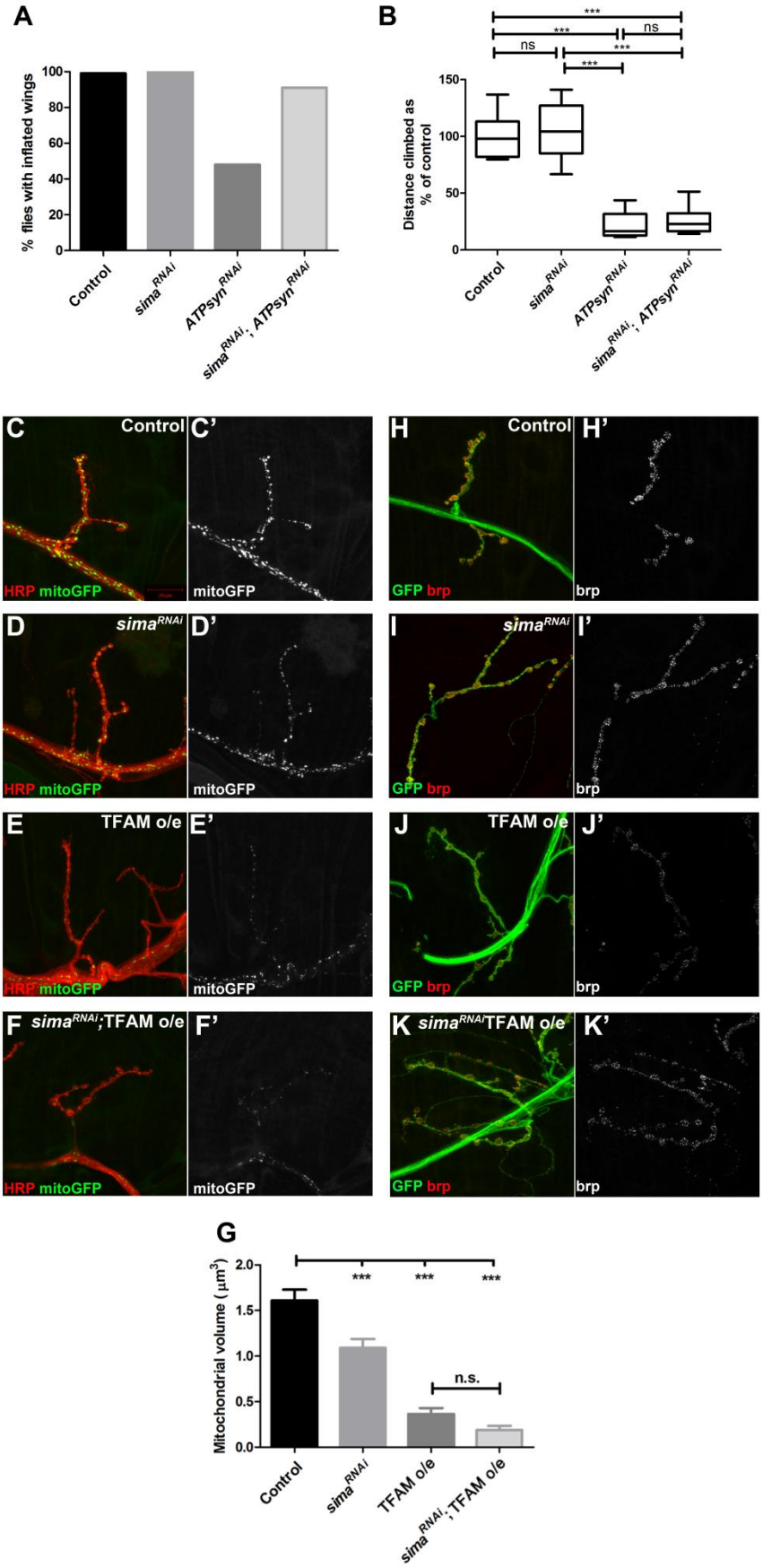
A
% flies with inflated wings
100
80
60
40
20
0
Control
sima RNAi
ATPsyn RNAi
sima RNAi; ATPsyn RNAi
B
Distance climbed as % of control
150
100
50
0
***
ns
***
***
ns
***
Control
sima RNAi
ATPsyn RNAi
sima RNAi; ATPsyn RNAi
C Control
C'
HRP mitoGFP
mitoGFP
H Control
H'
GFP brp
brp
D sima RNAi
D'
HRP mitoGFP
mitoGFP
I sima RNAi
I'
GFP brp
brp
E TFAM o/e
E'
HRP mitoGFP
mitoGFP
J TFAM o/e
J'
GFP brp
brp
F sima RNAi;TFAM o/e
F'
HRP mitoGFP
mitoGFP
K sima RNAiTFAM o/e
K'
GFP brp
brp
G
Mitochondrial volume (µm3)
2.0
1.5
1.0
0.5
0.0
***
***
***
n.s.
Control
sima RNAi
TFAM o/e
sima RNAi;TFAM o/e